JOURNAL OF MATERIALS SCIENCE 29 (1994) 5054–5058

Modified mixed oxide perovskites $0.7Sr(Al_{1/2}B_{1/2})O_3 \cdot 0.3LaAlO_3$ and $0.7Sr(Al_{1/2}B_{1/2})O_3 \cdot 0.3NdGaO_3$ ($B = Ta^{5+}$ or Nb^{5+}) for high-T_c superconductor substrate applications

RUYAN GUO, P. RAVINDRANATHAN, U. SELVARAJ, A. S. BHALLA, L. E. CROSS, RUSTUM ROY
Materials Research Laboratory, The Pennsylvania State University, University Park, PA 16802, USA

Single-crystal fibres of modified strontium aluminium tantalum oxide $(1-x)Sr(Al_{1/2}Ta_{1/2})O_3 \cdot xLaAlO_3$ (SAT·LA) and $(1-x)Sr(Al_{1/2}Ta_{1/2})O_3 \cdot xNdGaO_3$ (SAT·NG), and modified strontium aluminum niobium oxide $(1-x)Sr(Al_{1/2}Nb_{1/2})O_3 \cdot xNdGaO_3$ (SAT·NG) and $(1-x)Sr(Al_{1/2}Nb_{1/2})O_3 \cdot xLaAlO_3$ (SAN·LA) were grown using a laser-heated pedestal growth technique. 0.7SAT·0.3LA grows congruently and retains a twin free simple cubic perovskite structure (as the SAT) when cooled down to room temperature. 0.7SAT·0.3LA crystals have a moderate dielectric constant ($\kappa = 21.7$) and low dielectric loss ($\tan\delta = 7.5 \times 10^{-5}$) at 10 kHz and 90 K. The reduction problem of Ta^{5+} is eliminated (which is common in the case of SAT growth). 0.7SAT·0.3NG and 0.7SAN·0.3NG have lower melting temperatures and crystal growth is easier. $NdGaO_3$ addition to the SAT and SAN enhances the potential of SAT and SAN as large-area substrates for high-T_c superconductor growth. However, the dielectric constants increased from $\kappa \simeq 12$ to $\kappa \simeq 16$(0.7SAT·0.3NG) and from $\kappa \sim 18$ to $\kappa \sim 23$ (0.7SAN·0.3NG) as a result of $NdGaO_3$ incorporation.

1. Introduction

One of the recent interests in high-T_c superconductor (HTSC) thin films has been to develop suitable substrate materials for microwave device applications. The ideal substrate for such application should satisfy the following condition [1]: (i) the lattice constants (or the atomic arrangement) of the substrate should be closely matched to the HTSC thin films; (ii) the substrates should have a low dielectric constant and dielectric loss at low temperature; (iii) the substrates should not have any phase transitions that create micro-twins; and (iv) if possible, the substrates should be readily prepared in large sections that often requires materials of moderate melting points suitable for Czochralski growth. Various single crystals such as $SrTiO_3$, $LaAlO_3$, $LaGaO_3$, Al_2O_3, MgO and yttrium-stabilized ZrO_2 (YSZ) have been used as substrates for the HTSC thin films [2–4]. However, these substrates satisfy only part of the above-mentioned conditions.

We have been studying the crystal chemistry of perovskite oxides for quite some time and we have proposed many complex oxides for substrate applications [5, 6]. The results of our approaches presented in this paper are basically two-fold: (i) to control the twinning problem in $LaAlO_3$ by introducing chemical modification to stabilize the cubic phase at room temperature, and (ii) to lower the melting temperatures of the complex perovskite single crystals $Sr(Al_{1/2}Ta_{1/2})O_3$(SAT) and $Sr(Al_{1/2}Nb_{1/2})O_3$(SAN) as a follow-up of our previous work [7].

$LaAlO_3$ is a rhombohedrally distorted perovskite ($A^{3+}B^{3+}O_3$ type) with a pseudo-cell of $a = 0.3789$ nm, $\gamma = 90.12°$ and has a ferroic phase transition at $\sim 435\,°C$ [8] that results in highly twinned crystals [9, 10]. Although the La^{3+} ion generally prefers the 12-coordination site, there is a trend for the 9-coordination. The distortion in the LaO_{12} polyhedron is brought about by a slight displacement of the oxygen atoms away from the ideal positions of the cubic perovskite form, as is more clearly shown in other $[\text{rare-earth}]^{3+}AlO_3$ family members when the A-site cation radius become even smaller, e.g. in the case of $PrAlO_3$ [11, 12].

In fact, no ideal cubic perovskite structure has been reported in ternary compounds of the $[A]^{3+}[B]^{3+}O_3$ type [13]. Fig 1 presents a classification of $[A]^{3+}[B]^{3+}O_3$ type compounds according to the constituent ionic radii (8-coordination cation radii were used for A-site cations) focusing on the pervoskite region. The $[LaAlO_3]$ and $[GdFeO_3]$ are the only perovskite-like regions in the figure. For aluminate

0022–2461

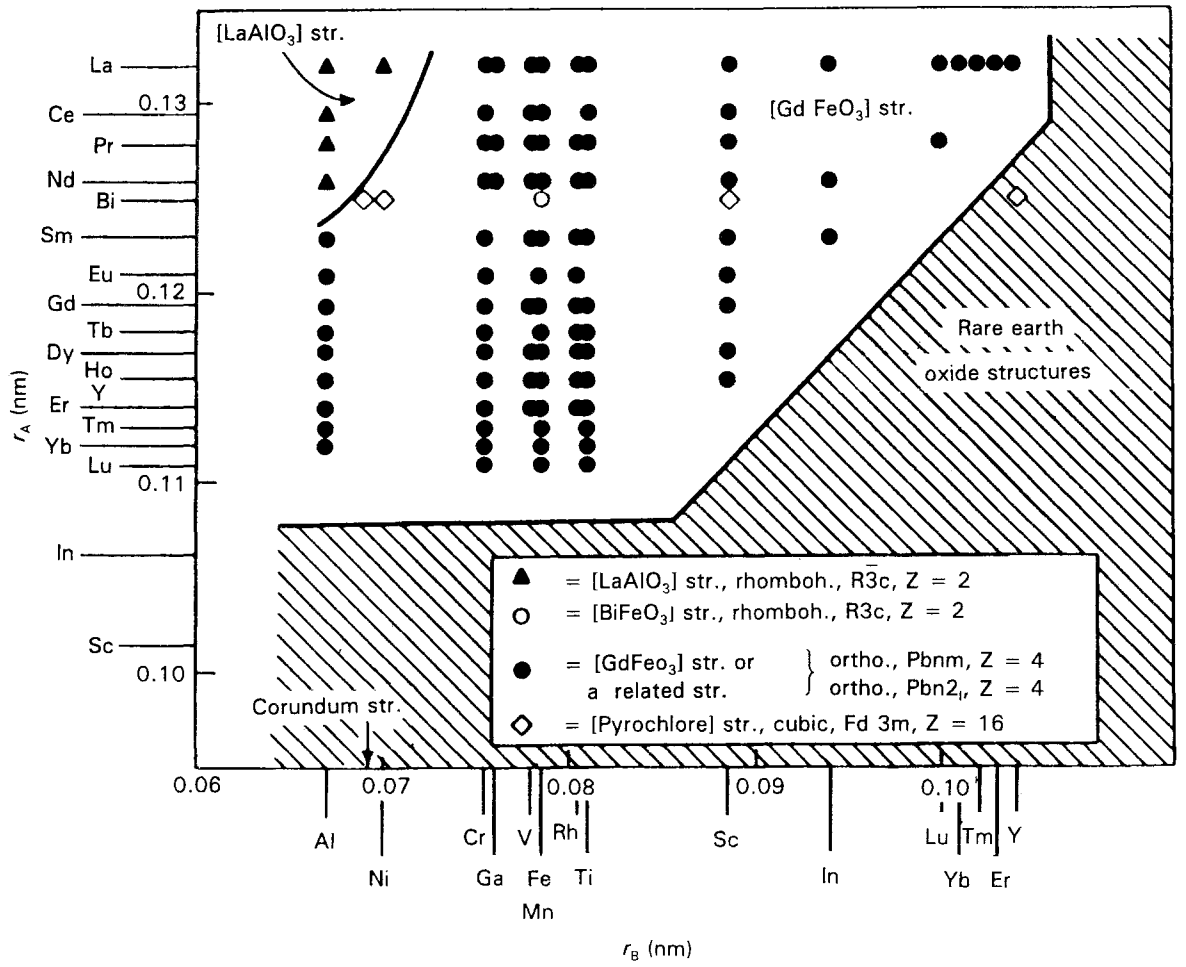

Figure 1 Structure field map for $A^{3+}B^{3+}O_3$ perovskites [12].

compounds, the largest A^{3+} cation, La^{3+}, has rhombohedral symmetry and the other $[A]^{3+}[Al]^{3+}O_3$ compounds have even lower symmetry.

It is therefore our approach in this study to introduce "balanced" cation substitution simultaneously in the A- and B-sites by forming crystalline solutions of known end members to increase the average cation size at the A-site to stabilize the 12-coordination of that position and consequently the cubic perovskite structure. Recently, Mateika and co-workers [4, 14] reported mixed rare-earth aluminium perovskites obtained by coupled substitution of {[Sr, Ca], [Ta, Nb]} and the crystal growth thereof by the Czochralski method. Such mixed crystals are twin-free when the cubic symmetry is obtained. One of the compositions they studied, $(La_{0.289}Sr_{0.709})(Al_{0.646}Ta_{0.356})O_3$, may be considered as a solid solution of two end members, $LaAlO_3$ and $Sr(Al_{1/2}Ta_{1/2})O_3$ (SAT). We have reported the growth of single-crystal fibres of the latter by the laser-heated pedestal growth technique [7].

SAT and SAN are potential substrates for HTSC and have a near-ideal lattice fit to them, excellent thermal expansion compatibility and desirable dielectric properties. The dielectric constant κ of SAT was found to be ~ 12, one of the lowest reported in the oxide perovskite family. However, both of them have relatively high melting temperatures (SAT: 1900 [15] or 1908 $\pm$ 25 [7], SAN: 1790 [15] or 1739 $\pm$ 10 [7]) so they cannot be grown using platinum crucibles by the Czochralski growth technique. Reduction of Nb^{5+} or Ta^{5+} was also found to be intrinsic in these crystals grown in air. By forming crystalline solutions with compounds of low melting temperatures, it was hoped that the crystalline solution would result in lower melting temperatures and consequently avoid the reduction problem and permit growth in platinum. We have measured the melting temperatures of various oxide perovskites [6] and the refractory character of this family is generally well known. $NdGaO_3$ proved to be an exception; it was found to have a melting temperature of $\sim 1484 \pm 24\,^{\circ}C$, and it was therefore selected as an end member of the crystalline solution series with SAT and/or SAN for the present studies. $NdGaO_3$ has the $[GdFeO_3]$ structure with orthorhombic symmetry, as do a majority of the $[A]^{3+}[B]^{3+}O_3$ type compounds (Fig. 1). No twinning problems were reported in this material. YBCO thin films of superior quality were deposited on $NdGaO_3$ as compared to the YBCO film deposited on an $LaAlO_3$ substrate. However, the high dielectric loss in the $NdGaO_3$ is a limiting factor for the YBCO film applications in microwave devices and resonators.

This paper reports an approach in which by forming the crystalline solutions between selected end members the specific properties are modified to meet the requirements of the HTSC thin films for microwave device applications. The selected crystalline solution phase $0.7Sr(Al_{1/2}Ta_{1/2})O_3 \cdot 0.3LaAlO_3$, $0.7Sr(Al_{1/2}Nb_{1/2})O_3 \cdot 0.3LaAlO_3$, $0.7Sr(Al_{1/2}Ta_{1/2})O_3 \cdot 0.3NdGaO_3$ and $0.7Sr(Al_{1/2}Nb_{1/2})O_3 \cdot 0.3NdGaO_3$ (referred

to in their shorthand forms as SAT-LA, SAN-LA, SAT-NG and SAN-NG, respectively, in the paper) and their single-crystal growth, structure and properties are reported in this paper.

2. Experimental procedure

2.1. Sample preparation

$La(OH)_3$, $SrCO_3$ and the respective oxides were used as starting materials. The purity of the starting materials was about 99.9% or better. The starting materials were weighed in the right stoichiometric ratio and thoroughly mixed using a ball mill with a carrier solvent such as ethanol. The resulting mixture was dried at 100 °C and fired at 1100 °C for 12 h. The sample was then reground and fired at 1400 °C for an additional 12 h. X-ray powder diffraction (XRD) was used to identify the products after each step of the processing. Finally, the sample was reground and fired at 1500 °C for 6 h.

The calcined powders were sieved through 325 mesh screen. A 2 wt % polyvinyl alcohol (PVA) aqueous solution was added as binder. The calcined powders containing PVA binder were then pressed as pellets. The pellets were sintered at 1500 to 1625 °C, depending on the compositions, for 6 h.

2.2. Melting point determination

Melting points were determined using a strip furnace and optical pyrometers. The heating element consisted of a V-shaped ribbon of iridium metal clamped between two water-cooled brass electrical contacts. The current through the strip was controlled by two variable a.c. transformers connected with a vernier control arrangement for better temperature control. The notch of the V acts as a black-body cavity. This extremely simple furnace, designed in 1930, was used extensively in the early work on perovskites in the 1950s [16].

The samples, having been determined to be a single phase by X-ray diffraction, were placed in the notch of the strip in the form of a small amount (pinhead) of granular powder. The temperatures of the sample and the strip were monitored simultaneously using three optical pyrometers through which the onset of melting was observed. Each measurement was repeated three times with fresh samples and refined temperature scales. A total of nine readings were taken for each sample by three independent operators and pyrometers. The average melting temperature was obtained along with the estimation of the precision of these measurements after rejecting the lowest and highest points.

2.3. Laser-heated pedestal growth technique

The laser-heated pedestal growth (LHPG) method was used to grow single-crystal fibres of modified compositions. The LHPG equipment used in this investigation consisted of a power source (water-cooled, tunable flowing gas CO_2 55 W laser), an optical layout, and a growth section. The alignment, seeding and growth were visually imaged outside the growth chamber by a short focal-length telescope which was in line with a CCD camera. Molten-zone temperature during a stable growth was monitored using an optical pyrometer focusing telescope with a resolution of linear dimension 0.1 mm. Further detailed description can be found elsewhere [17, 18].

3. Results and discussion

The X-ray powder diffraction patterns of the powder calcined at 1500 °C showed the presence of only a single phase. All four modified compositions were found to have the ideal simple cubic structure after crystallization as determined by the X-ray powder diffraction technique on the respective crystals. The crystallographic structure and lattice parameters are listed in Table I. Ceramic samples of SAT-NG (sintered at 1625 °C for 6 h) showed an ordered cubic structure that yielded a double cell with $a = 0.77732$ nm. Similarly, the SAN-NG ceramic sample (sintered at 1575 °C for 6 h) also has the ordered structure with a double unit cell of $a = 0.77647$ nm. The geometrical density of all the sintered samples was more than 91% of the theoretical density when the sintering temperature was 1600 °C.

Our results further confirmed the report of Mateika *et al.* [4] that the ideal cubic phase can be formed in (La, Sr) (Al, Ta)O_3 compounds. It is interesting to notice that similar substitutions using [Ca, Ta] instead of [Sr, Ta] did not produce a compound with cubic structure. The average A-site cation radius of the [Ca, Ta] substitution is smaller than that of $LaAlO_3$ (ionic radii of Ca^{2+}, La^{3+} and Sr^{2+} are 0.114, 0.1185, and 0.127 nm, respectively) [20, 21]; therefore no stabilization effect on the 12-coordination A-site can be expected.

The existence of cubic symmetry for the compound of SAT-NG and SAN-NG may be due to the fact that Ga^{3+} is of almost the same cation size as Ta^{5+}/Nb^{5+}. Slight reduction in the A-site cation size is accompanied by a slight increase of the B-site cation size and thus the cubic structure of SAN or SAT stays intact.

The melting temperatures as determined using the strip furnace melting and the optical pyrometer, along

TABLE I Symmetry and lattice parameters of the modified compounds determined by X-ray diffraction.

Composition	Symmetry	Lattice constant (nm)	Density ($g\,cm^{-3}$)
SAT	Cubic	$a = 0.38952$	6.731
SAN	Cubic	$a = 0.38995$	5.476
$LaAlO_3$	Rhomb.	$a = 0.3789$, $\gamma = 90.12°$	6.532
$NdGaO_3$	Ortho. [19] [$GdFeO_3$] structure	$a = 0.5426$, $b = 0.5502$ $c = 0.7706$ (pseudo cell $a_0 = 0.3860$)	7.561
SAT-LA	Cubic	$a = 0.38727$	6.628
SAN-LA	Cubic	$a = 0.38634$	5.798
SAT-NG	Cubic	$a = 0.38866$	6.965
SAN-NG	Cubic	$a = 0.38790$	6.130

with the observed stable growth zone temperature during LHPG, are listed in Table II. It is especially interesting that $NdGaO_3$ addition to SAT and SAN reduced the melting point as expected.

Single crystals of SAT-LA, SAT-NG, SAN-LA and SAN-NG were grown by the LHPG technique using the ceramic rods as both seed and feed materials. All growth was performed in air. The temperatures required for the growth of SAT-LA was somewhat lower (by $\sim 100\,^{\circ}C$) than that for the growth of SAT; however, the crystals as grown were transparent and colourless. The reduction problems found earlier in SAT growth were eliminated. Crystal fibres of $\sim 500\,\mu m$ diameter did not show any clear facet and cleavage characteristics. Single crystals of SAT-NG and SAN-NG were likewise easier to grow than their unmodified forms, as their respective melting temperatures were considerably lower and the stable growth melt zone during the LHPG growth was easier to maintain. Crystal fibres of SAT-NG and SAN-NG of ~ 400–$500\,\mu m$ diameter and 40 mm length were grown. The as-grown SAT-NG and SAN-NG both had a dark colour, with the SAT-NG being lighter and partially transparent. The colour of the crystals is believed to be due to the Ga^{3+} in the compound. As-grown SAT-NG and SAN-NG single-crystal fibres are shown in Fig. 2.

Dielectric properties of the ceramic samples were measured using a General Radio 1621 capacitance measurement system. A three-terminal measurement was carried out using an environmental-controllable sample holder. The stray capacitance, lead and contact resistance were corrected during the measurements by taking into account the open-circuit measurement. The edge corrections were made to the results by using an empirical equation obtained from a family of fused silica samples.

The dielectric constant κ and loss tangent of the modified samples were examined as functions of temperature and frequency. Table III summarizes the values obtained on ceramic samples at liquid nitrogen temperature and at 10 kHz. The dielectric property of the crystalline solution SAT-LA appeared to have maintained the dielectric features of the $LaAlO_3$ alone, though with the twin-free cubic structure resulting from the SAT end member. All $NdGaO_3$ end-member compounds have low dielectric loss ($< 5.1 \times 10^{-4}$); however, the dielectric constants of modified compounds appeared to be elevated by the addition of $NdGaO_3$. In general, all the compounds studied have comparable or lower dielectric constants and comparable dielectric loss to the rhombohedral $LaAlO_3$ simple perovskite.

Thermal expansion coefficients of the crystalline solution compounds were measured in comparison to the thermal properties of the YBCO superconductor and are listed in Table IV. Good thermal expansion matching was found in all NG end-member compounds. $LaAlO_3$ and modified SAT-LA samples,

TABLE II Melting temperatures of modified complex perovskites

Composition	M.p (°C) (strip furnace)	LPHG molten zone temp. (°C ± 0.5%)
$Sr(Al_{1/2}Ta_{1/2})O_3$	1908 ± 25	2049
$Sr(Al_{1/2}Nb_{1/2})O_3$	1739 ± 10	1862
$LaAlO_3$	2040 ± 9	
$NdGaO_3$	1484 ± 24	
0.7SAT·0.3$LaAlO_3$	1830 ± 22	1946
0.7SAT·0.3$NdGaO_3$	1767 ± 31	1832
0.7SAN·0.3$LaAlO_3$	1705 ± 20	
0.7SAN·0.3$NdGaO_3$	1582 ± 20	1775

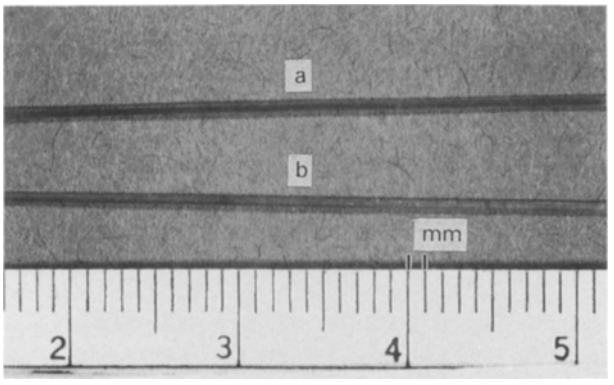

Figure 2 Single-crystal fibres of (a) SAT-NG and (b) SAN-NG grown by the laser heated pedestal growth technique.

TABLE III Dielectric properties of modified complex perovskites

Material	Value at 10 kHz, 90 K	
	K	tanδ
$LaAlO_3$	23	7.47×10^{-5}
$NdGaO_3$(77 K, 10 GHz) [22]	23	3.24×10^{-4}
$Sr(Al_{1/2}Ta_{1/2})O_3$	11.8	4.24×10^{-5}
$Sr(Al_{1/2}Nb_{1/2})O_3$	18.7	2.20×10^{-4}
0.7SAT·0.3$LaAlO_3$	21.7	7.47×10^{-5}
0.7SAN·0.3$LaAlO_3$	25.7	2.79×10^{-4}
0.7SAT·0.3$NdGaO_3$	16.0	4.25×10^{-4}
0.7SAN·0.3$NdGaO_3$	23.0	5.15×10^{-4}
1/3SAN·1/3SAT·1/3$NdGaO_3$	22.3	5.11×10^{-4}

TABLE IV Coefficient of thermal expansion measured by dilatometry technique (RT ~ 800 °C) [23]: $\Delta L/L_0 = A_0 + \alpha T + \beta T^2$

Material	$\alpha(\times 10^{-6\circ}C^{-1})$ at ~ 300 K	$\alpha(\times 10^{-6\circ}C^{-1})$, $\beta(\times 10^{-8\circ}C^{-2})$ (300–1050 K)
YBCO [24][a]	14 (a_a)	
	9 (a_b)	
	19 (a_c)	
	42 (a_v)	
YBCO ceramic	10.9	9.5
$LaAlO_3$//[1 $\bar{1}$ 0]	8.2	
//0 0 1]	6.4	
$Sr(Al_{1/2}Ta_{1/2})O_3$	9.7	8.9, 1.1
$Sr(Al_{1/2}Nb_{1/2})O_3$	8.5	6.5, 2.4
0.7$Sr(Al_{1/2}Ta_{1/2})O_3$·0.3$LaAlO_3$	7.7	
0.7$Sr(Al_{1/2}Nb_{1/2})O_3$·0.3$NdGaO_3$	10.8	
0.7$Sr(Al_{1/2}Ta_{1/2})O_3$·0.3$NdGaO_3$	8.8	6.3, 3.6
0.7$Sr(Al_{1/2}Nb_{1/2})O_3$·0.3$LaAlO_3$	9.5	

[a] Untwinned single crystal at 300 K

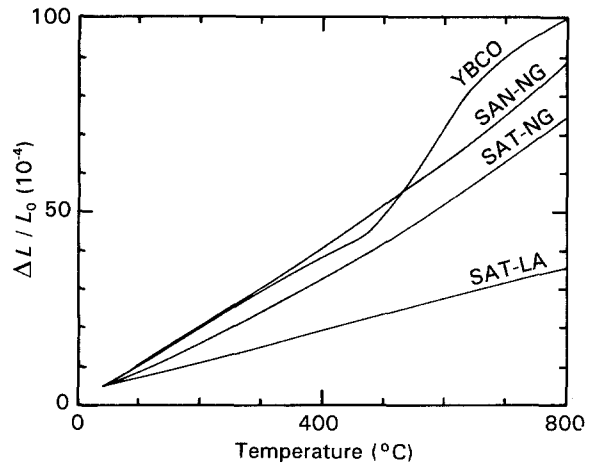

Figure 3 Thermal strains versus temperature as measured using the push-rod linear voltage differential dilatometer [23].

however, showed thermal expansion coefficients somewhat smaller than the ideal. There has been a report on the thermal expansion coefficient of $LaAlO_3$ as being $10 \times 10^{-6}\,°C^{-1}$ [25] and the discrepancies between our results and the reported values may be due to the different thermal annealing history of the samples. In our measurements, the $LaAlO_3$ crystal was annealed several times at temperature $\sim 800\,°C$ before thermal strain measurements were done, and also our results were reproducible. No structural phase transition was found in the measured temperature region for all the compositions listed. Plots of the thermal strains versus temperature as measured are shown in Fig. 3.

4. Conclusions

The ideal cubic perovskite structure can be stabilized in the case of $LaAlO_3$ by forming crystalline solution compositions with cubic $Sr(Al_{1/2}Ta_{1/2})O_3$ and $Sr(Al_{1/2}Nb_{1/2})O_3$. The mechanism of this type of stabilization is perhaps through introducing compensated cation substitution in the form of $[2La^{3+}] + [Al^{3+}] \rightarrow [2A^{2+}] + [B^{5+}]$ with the A^{2+} cation having a radius larger than that of La^{3+} and therefore stabilizing the 12-coordinated A-site. Crystalline solutions of SAT-LA maintained most of the dielectric and thermal properties of $LaAlO_3$ and gained the advantage of forming a twin-free simple cubic structure and improved lattice compatibility. $NdGaO_3$ is shown to be an effective end member to decrease the melting temperature of SAN and SAT without disturbing their simple cubic (twin-free) crystal structure. Dielectric constants of SAN and SAT with an addition of $NdGaO_3$ were increased; however, the dielectric loss factor still remained less than 5×10^{-4}. The results suggest that SAT-LA and SAN-LA are better candidates as substrate materials than $LaAlO_3$ because they have the twin-free cubic structure. Also the growth of SAT-NG and SAN-NG is comparatively convenient as they have relatively low melting temperatures together with relatively lower dielectric constants and ideal lattice constants and thermal compatibility with the YBCO superconducting material.

Acknowledgements

The authors thank Dr. S. Erdei and Professor. F. W. Ainger for the discussion on the subject. This work was supported by the Defense Advanced Research Projects Agency (DARPA) under contract DN 00014-90-J-4140.

References

1. H. M. O'BRYAN, P. K. GALLAGHER, G. W. BERKSTREKKER and C. D. BRANDLE, *J. Mater. Res.* **5** (1990) 183.
2. T. VENKATESAN, C. C. CHANG, D. DIJKKAMP, S. B. DGALE, E. W. CHASE, L. A. FARROW, D. M. HWANG, P. F. MICELI, S. A. SCHWARZ, J. M. TERASION, X. D. WU and A. INAM, *J Appl. Phys.* **63** (1988) 4591.
3. G. KOREN, A. GUPTA, E. A. GIESS, A. SEGMULLER, and R. B. LAIBOWITZ, *Appl. Phys. Lett.* **54** (1989) 1054.
4. D. MATEIKA, H. KOHLER, H. LAUDAN and E. VÖLKEL, *J. Cryst. Growth* **109** (1991) 447.
5. L. E. CROSS, R. ROY. R. GUO, J. SHEEN, A. S. BHALLA, F. W. AINGER and E. C. SUBBARAO, presented at Defence Advanced Research Projects Agency (DARPA) 3rd Annual High Temperature Superconductor Workshop, Seattle, Washington, September (1991).
6. R. GUO, J. SHEEN, A. S. BHALLA, F. AINGER, E. C. SUBBARAO and L. E. CROSS, presented at Defence Advanced Research Projects Agency and Office of Naval Research (DARPA/ONR) Workshop on substrate Materials for High-T_c Superconductors, Colonial Williamsburg, Virginia, February (1992).
7. R. GUO, A. S. BHALLA, JYH SHEEN, F. W. AINGER, E. C. SUBBARAO and L. E. CROSS, *J. Mater. Res* (in press).
8. E. A. WOOD, *Amer. Min.* **36** (1951) 768.
9. S. GELLER and V. B. BALA, *Acta Crystallog.* **9** (1956) 1019.
10. M. DAVIDSON, *Superconductor Industry* **5**(2) (1992) cover page.
11. R. D. BURBANK, *J. Appl. Cryst.* **3** (1970) 112.
12. O. MULLER and R. ROY, in "The Major Ternary Structural Families" (Springer, Berlin, 1974) p. 215.
13. F. S. GALASSO, in "Structure, Properties and Preparation of Perovskite-type Compounds" (Pergamon, Oxford, 1969) p. 10.
14. S. HAUSSÜHL and D. MATEIKA, *Cryst. Res. Technol.* **26** (1991) 481.
15. C. D. BRANDLE and V. J. FRATELLO, *J. Mater. Res.* **5** (1990) 2160.
16. M. L. KEITH and R. ROY, *Amer. Min.* **39** (1954) 1.
17. J. YAMAMOTO and A. S. BHALLA, *Mater. Res.* **24** (1989) 761.
18. R. GUO, A. S. BHALLA and L. E. CROSS, *J. Appl. Phys.* **75** (1994) 4704.
19. S. GELLER, *Acta Crystallogr.* **10** (1957) 243.
20. R. D. SHANNON and C. T. PREWITT, *ibid.* **B25** (1969) 925
21. *Idem, ibid.* **B26** (1970) 1046.
22. T. KONAKA, M. SATO, H. ASANO and S. KUBO, *J. Supercond.* **4** (1991) 283.
23. R. GUO, J. POVOA and A. S. BHALLA, *Mater. Res. Lett.* in press.
24. HOYDOO YOU, U. WELP and Y. FANG, *Phys. Rev.* **B43** (1991) 3660.
25. R. RAMESH, A. INAM, W. A. BONNER, P. ENGLAND, B. J. WILKENS, B. J. MAEGHER, L. NAZAR, X. D. WU, M. S. HEDGE, C. C. CHANG, T. VANKATESAN and H. PADAMSEE, *Appl. Phys. Lett* **55** (1989) 1138.

Received 4 August
and accepted 14 September 1993